# Recovering Shape and Reflectance Model of Non-lambertian Objects from Multiple Views

Tianli Yu, Ning Xu and Narendra Ahuja
*Electrical and Computer Engineering Department*
*University of Illinois at Urbana-Champaign*
*{tianli, ningxu, ahuja}@vision.ai.uiuc.edu*

## Abstract

*This paper proposes an algorithm to simultaneously estimate both the 3D shape and parameters of a surface reflectance model from multiple views of an object made of a single material. The algorithm is based on a multiple view shape from shading method. The shape of the object is represented by a triangular mesh. The Phong reflectance model is used to model the surface reflectance. We iteratively find the shape and reflectance parameters that best fit all input images. The estimates of shape and reflectance model are gradually refined by subdividing triangles in the mesh into smaller ones. The estimation takes into account both self-occlusion and self-shadowing. Analysis shows that the accuracy of reflectance estimation is limited by the triangle size in the shape model. We also propose to use Richardson extrapolation to overcome this and further refine the reflectance model estimate. The estimated 3D shape and reflectance model can be used to render the same object from different viewing directions and under different lighting conditions. Experimental results on both synthetic and real objects are given.*

## 1. Introduction

A bottleneck in the creation of realistic scenes for computer graphics is often the high cost of acquiring models of real objects, including 3D shapes, surface reflectance properties and lighting conditions. In this paper, we present an algorithm to acquire both the 3D shape and surface reflectance properties simultaneously from images of an object taken from multiple viewpoints. The result is a set of shape and reflectance parameters that can be used to render the object from new viewpoints and under different lighting conditions.

### 1.1 Related works

3D reconstruction and surface reflectance estimation from images have usually formed two separate problems in computer vision for many years. For 3D reconstruction, the use of simpler reflectance model, namely the lambertian model, is common. Lambertian property makes a surface appears identical from all viewing directions, and therefore simplifies matching based 3D reconstruction. Solutions for general non-lambertian scenes have only been pursued recently. For example, Jin et.al [1] propose to use the rank constraint of radiance tensor as the discrepancy measure for correspondences. Their method can handle objects with high specularity. Shape from shading (SFS) and photometric stereo methods make use of shading information to recover 3D shape. These methods usually assume that surface reflectance properties are known. Much work on shape from shading is based on the lambertian model, uses a single view, or assumes simple lighting conditions [2]. In general, single view shape from shading problem is ill-conditioned, more so for non-lambertian objects with unknown reflectance, and its solution relies on strong regularization. Multiple view shape from shading methods have been used to improve the conditioning and have also enabled recovery of surface albedo under lambertian reflectance [3, 4]. Similar research is also done in the context of the fusion of SFS and shape from motion (SFM) [21]. Under lambertian assumption, SFS and SFM can be applied separately and the results fused at a later stage. For more general reflectance, SFS and SFM are intertwined through BRDF and the problem need to be treated in an integrated manner. By controlling lighting conditions, photometric stereo and related methods improve the conditioning of the problem while avoiding the correspondence issue. Lee & Kuo [5] use photometric stereo in conjunction with a polygonal mesh, instead of surface normal, as the surface model, and the

Torrance-Sparrow reflectance model to recover the shape. Hertzmann and Seitz [6] place several reference spheres with materials similar to those of the object into the scene to reconstruct the 3D shape of the object (lambertian or non-lambertian) from a single view using photometric stereo. However, the needs for the control of lighting and calibration spheres restrict the method's applicability. Further, none of these methods consider self-shadowing.

In computer graphics, estimation of reflectance properties from images, through Bidirectional Reflectance Distribution Function (BRDF), is referred to as an "inverse rendering" problem. Much of the work on this is done assuming known 3D geometry. Marschner [7] proposes a method to acquire dense samples of BRDF from images of a single material surface. Debevec et al. [8] estimate the reflectance field of a human face using a controlled light stage. Love [9] estimates the reflectance model for outdoor scenes under natural illumination. Apricio et al. [10] propose a method to acquire phong reflectance model from range and intensity images. Ramamoorthi and Hanrahan [11] give taxonomy of different inverse rendering approaches and propose a general signal processing framework to estimate both illumination and BRDF.

In image based modeling, often neither the 3D structure nor the reflectance model of the object is known. Most previous work estimates these characteristics in two separate steps. Sato et al. [12] first construct a 3D model of the object by merging the range images from different views. Using the model, they separate the diffuse and specular color components and estimate the corresponding reflectance parameters. Kim et al. [13] first estimate the Torrance-Sparrow model using a sample sphere made of the same material as the object. And then use this model and photometric stereo to recover the 3D object shape. Clearly, a more desirable formulation would result if the two steps are integrated.

### 1.2 Contributions of this paper

This paper is aimed at simultaneous recovery of both 3D shape and surface reflectance properties from multiple calibrated views of a non-lambertian object. We assume that the object is made from a single material, and lighting distribution is known or estimated separately. We neglect any inter-reflections between different parts of the object. The main features and contributions of this paper are as follows:

a. We incorporate multiple view information so that the shape and reflectance estimation problems become well-conditioned.
b. We take into account the effects of self-occlusions and self-shadows.
c. We use information about object silhouette present in the multiple views, which gives a good initial shape estimate and also helps predict occlusion.
d. We avoid potentially poor scaling among shape and reflectance parameters by iterating between two separate optimization steps.
e. We extrapolate the reflectance model parameters estimated from different scales to further refine the estimation.

This paper is organized as follows. Section 2 poses the problem as one of minimization over shape and reflectance parameters. Section 3 proposes an iterative and multi-scale method to minimize the cost function; various issues such as shadows, occlusions, initialization, and reflectance parameters extrapolation are also discussed. Section 4 gives experiment results on real and synthetic images. Section 5 presents conclusions and directions of future work.

## 2. Problem formulation

Our proposed method extends shape from shading algorithms to incorporate multiple views. It is based on the "synthesis and analysis" idea which is also used in [14] for specular surface reconstruction. It synthesizes the images of the object from different viewpoints based on the current shape and reflectance model, and compares them with the observed images. Then it gradually improves the shape and reflectance to better match the observations.

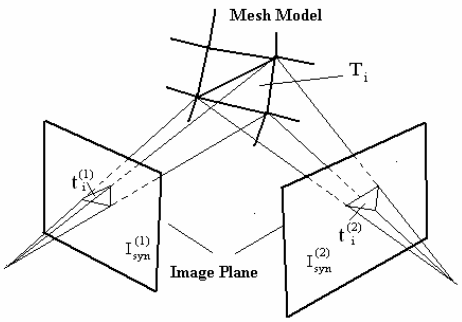


**Fig. 1. Synthesize images from a mesh model.**

As shown in Fig. 1. We represent the object shape with a triangular mesh having vertices $V = \{V_k \mid k = 1...m\}$. Each triangular facet on the object surface is represented as the collection of its three vertices.

$$T_i = < V_{i1}, V_{i2}, V_{i3} > \quad (1)$$

The object's surface $S_{obj}$ is the union of all the triangles on the mesh. We use $\vec{V}$ and $\vec{B}$ to denote the

vectors of shape parameters and reflectance model parameters respectively.

If $\pi_j : R^3 \to R^2$ denote the projection transform from 3D world coordinate to j[th] image plane, then the projected patch of $T_i$ on the j[th] synthesized image is:

$$t_i^{(j)} =< v_{i1}^{(j)}, v_{i2}^{(j)}, v_{i3}^{(j)}, R_i^{(j)}(\vec{n}_i, \vec{e}_i^{(j)}, \vec{B}, \vec{L}) > \quad (2)$$

where $v_{im}^{(j)} = \pi_j(V_m), m = 1,2,3$, and $R_i^{(j)}(\vec{n}_i, \vec{e}_i^{(j)}, \vec{B}, \vec{L})$ denotes the reflectance value of the triangle in the jth image, computed from the triangle's normal direction $\vec{n}_i$, viewing direction $e_i^{(j)}$, reflectance model $\vec{B}$, and all the light sources $\vec{L}$ that can illuminate the triangle. Here we assume every triangle has a uniform reflectance value in each view. The synthesized image is the union of the projected patches of all visible triangles,

$$I_{syn}^{(j)} = \bigcup_{Ti\ is\ visible\ in\ jth\ view} t_i^{(j)} \quad (3)$$

The observed patch corresponding to $T_i$ in the j[th] input image, $o_i^{(j)}$, can be expressed as the quadruplet

$$o_i^{(j)} =< v_{i1}^{(j)}, v_{i2}^{(j)}, v_{i3}^{(j)}, I_i^{(j)} > \quad (4)$$

where $I_i^{(j)}$ is the average intensity value of $o_i^{(j)}$ on j[th] input image $I^{(j)}$.

We define the error between $t_i^{(j)}$ and $o_i^{(j)}$ as the difference of $R_i^{(j)}$ and $I_i^{(j)}$, weighted by the number of pixels $q(o_i^{(j)})$ in $o_i^{(j)}$

$$err(t_i^{(j)}, o_i^{(j)}) = (R_i^{(j)} - I_i^{(j)}) \cdot q(o_i^{(j)}) \quad (5)$$

We also define a cost function $C$ to represent the difference between synthetic and observed images as the sum of the squared error in (5) over all visible triangles and all input views.

$$C(\vec{V}, \vec{B}) = \sum_{j=1}^{p} \sum_{Ti\ visible\ in\ jth\ view} [err(t_i^{(j)}, o_i^{(j)})]^2 \quad (6)$$

Our goal is to find a set of optimal shape and reflectance model parameters $< \vec{V}^*, \vec{B}^* >$ that minimize the cost function:

$$< \vec{V}^*, \vec{B}^* >= \arg\min\{C(\vec{V}, \vec{B})\} \quad (7)$$

# 3. Algorithms and implementation details

## 3.1 Shape parameterization

Shape parameters $\vec{V}$ consist of the majority of parameters to be optimized. To reduce the number of such parameters, we represent the vertices of our triangular mesh model in spherical coordinates with the origin inside the object (the origin is manually selected). For each vertex in the model, we fix the azimuthal and polar components and allow the vertices to move only in radial directions. Each vertex thus has only 1 degree-of-freedom along the vector from the origin. This will reduce the number of parameters by a factor of 3. However, this simplification restricts our mesh model to represent only star-shaped objects (where no two points on the object surface have the same pair of azimuthal and polar components). This star-shape constraint will help avoid vertices clustering together during the shape optimization process.

## 3.2 Reflectance model

We choose the Phong reflectance model [15] as the parametric reflectance model, since it is simple to compute, and most widely used in computer graphics. In Phong model, the reflectance of a surface patch under a directional light source $L_k$ can be computed as

$$R_i^{(j)}(\vec{n}, \vec{e}, \vec{B}, L_k) = |L_k| \cdot [k_d(\vec{n} \cdot \vec{l}_k) + k_s(\vec{r} \cdot \vec{e})^{\alpha}] \quad (8)$$

where $k_d$ and $k_s$ are the diffuse and specular coefficients and $\alpha$ is the Phong exponent. $\vec{r}$ is the reflection vector which is at the mirror position of light direction $\vec{l}$ with respect to surface normal. The reflectance of the patch under a group of light sources is the summation of the reflectance values from each light source:

$$R_i^{(j)} = \sum_{k=1}^{N_l} R_i^{(j)}(\vec{n}, \vec{e}, \vec{B}, L_k) \quad (9)$$

Sometimes the Phong model parameters are normalized such that $k_d + k_s = 1$. However, we will not do this in order to allow a global scaling factor from illumination estimation. Hence we need to estimate three parameters for the reflectance model.

## 3.3 Iterative optimization framework

Our cost function (6) has two sets of parameters, reflectance parameters $\vec{B}$ and shape parameters $\vec{V}$, whose interdependency leads to chicken-and-egg problem. Usually, this problem is resolved by using iterative methods, as done by Nayar et al. in [16] for solving shape from inter-reflection problem. Another reason for using iterative methods is the large difference in the role played by these two parameter sets. $\vec{B}$ is constrained over all the facets while $\vec{V}$ is constrained only locally. If we were to include them into a single optimization procedure, we will need to carefully choose a proper scale of these parameters in

order to avoid poor-conditioning. Hence, it is convenient to minimize them separately and interleave the optimization processes, as shown in Fig. 2

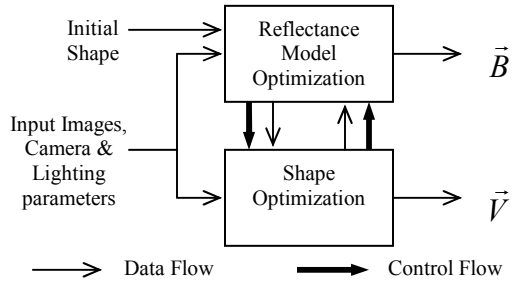


**Fig. 2. Flow chart of the iterative algorithm**

In Fig. 2, we start with an initial shape of the object, i.e. $\vec{V}_0$, and minimize the cost function to find a better $\vec{B}$. Then we fix $\vec{B}$ and refine $\vec{V}$. The whole process continues until the cost function in (6) no longer decreases or the progress of decrease is small. Since in both shape optimization and reflectance optimization we are minimizing a single cost function which is lower bounded by zero, the iterative process is guaranteed to converge.

We treat the minimization of cost function $C(\vec{V}, \vec{B})$ as a non-linear least square problem and obtain a solution by Trust Region Reflective Newton (TRRN) method [17]. Each iteration in the optimization involves approximate solution of a large linear system using the method of preconditioned conjugate gradients (PCG). It requires knowledge of the derivative of the error in (5) with respect to each parameter. For reflectance parameters, this can be computed using finite differencing. To compute directly the derivative with respect to the shape parameters is very costly. Strictly speaking, we need to re-project the mesh model in order to compute each term. We use an approximate solution instead. If we take the derivative of (5) with respect to $k^{th}$ shape parameter, we get:

$$\begin{aligned} \frac{\partial err}{\partial V_k} &= \frac{\partial \{[\, R_i^{(j)} - I_i^{(j)}] \cdot q(o_i^{(j)})\}}{\partial V_k} \\ &= \frac{\partial R_i^{(j)}}{\partial V_k} \cdot q(o_i^{(j)}) - \frac{\partial I_i^{(j)}}{\partial V_k} \cdot q(o_i^{(j)}) \\ &+ [R_i^{(j)} - I_i^{(j)}] \cdot \frac{\partial q(o_i^{(j)})}{\partial V_k} \end{aligned} \tag{10}$$

The derivative $\partial R_i^{(j)} / \partial V_k$ can be computed using finite differencing, $\partial I_i^{(j)} / \partial V_k$ can be approximated using the observed image gradient at the center of the observed patch $o_i^{(j)}$ in the vertex moving direction, and $\partial q(o_i^{(j)}) / \partial V_k$ can be approximated using the area change of the observed patch, all with respect to change in the location of the $k^{th}$ vertex.

### 3.4 Handling self-occlusion and self-shadowing

In (6), for every image, we need to compute the sum of the squared errors only over the visible triangles. Our algorithm ensures this by checking the triangle's visibility based on the current estimate of the shape at each step of the minimization process.

We also account for self-shadowing in a similar manner. For each discrete directional light source, we use orthographic projection to project the mesh model onto the image plane perpendicular to the light direction. Then all the invisible triangles are in the shadow area of that light source. For triangles that are partially visible, we compute the ratio between the visible triangle area and the projected triangle area, and scale the light source intensity in (8) with the ratio when computing the reflectance of those triangles.

### 3.5 Choosing initial shape

For a local optimization method, a good initial estimate is very important. We use the visual hull computed from the multiple silhouettes as the initial shape. Silhouette in each image can be obtained via image segmentation, or background subtraction. Visual hull gives a quite near initialization and helps avoid false positive of "un-occluded" areas (occluded areas interpreted as not occluded) in the initial iterations, since no possible shape of the object can have portions outside the visual hull. The visual hull also serves as the outer bound of the object shape during minimization.

### 3.6 Multi-scale shape minimization and Richardson extrapolation

Through iterative reflectance and shape optimization, we are able to find simultaneously a set of reflectance and shape parameters that minimize the cost function in (6). However, the TTRN method may only find a local minimum. A common solution to this problem is multi-scale analysis. Accordingly, we first optimize the shape and reflectance parameters using a coarse triangle mesh. Then we subdivide each triangle into four small triangles and start optimization at a finer scale. This multi-scale method will also decrease the total amount of computation for the algorithm.

After the optimization converges at each scale, we will get a set of estimated reflectance parameters. These parameters are based on the assumption that

each patch on the surface is approximated using a triangle facet, and therefore has a single surface normal and constant intensity value. The validity of this assumption increases as the triangle size decreases. However, recursive decomposition of the triangles leads to a stage where either the computational cost is too high to be acceptable, or the triangles are so small that their projection onto the image plane is smaller than a pixel. In this situation, Richardson Extrapolation [18] can be used to gain further accuracy.

The idea is that if we have more than two values of a parameter obtained at different scales, we can extrapolate the data to get an estimation of the parameter when the scale goes to zero. Since we are approximating the surface normal inside a triangle using a single normal, the error introduced by the approximation is proportional to the size of the triangles. This size can be represented as the square root of the average area of all the triangles in the mesh. We denote this value by the scale parameter $h$. Then the estimated reflectance model parameters can be written as a function of $h$. We use a Taylor series expansion of this function up to the first order to obtain:

$$\vec{B}(h) = \vec{B}(0) + \vec{B}'(0) \cdot h + O(h^2) \qquad (11)$$

If we approximate $\vec{B}(h)$ as a linear function, we can solve $\vec{B}(0)$ by two values. Suppose we estimate the reflectance model at scale $h$ to obtain $\vec{B}(h)$. A subdivision of triangles will gives another estimate $\vec{B}(h/2)$. Then $\vec{B}(0)$ can be obtained by extrapolation

$$\vec{B}(0) = 2\vec{B}(h) - \vec{B}(h/2) \qquad (12)$$

(12) approximates the reflectance parameters for the case when the scale parameter $h$ goes to zero, which means our estimation can extend beyond the size limit of the triangular mesh. This gives another advantage of using multi-scale analysis.

## 4. Experiments

### 4.1 The mouse surface data set

The mouse surface data set was captured with a Sony DSC-F717 digital camera. A computer mouse was placed on a table together with a calibration pattern. All the objects were put in a dark room illuminated by two distant light sources to minimize ambient light. Images of the mouse and calibration pattern were taken using fixed intrinsic parameters from different directions (Fig. 3)

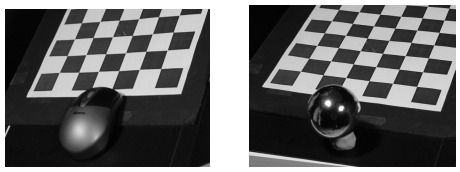

**Fig 3. Two images of the experimental setup**

A mirror sphere was also placed at the mouse position to measure the illumination distribution (Fig.3). Camera parameters were estimated from the calibration pattern using the toolbox described in [19]. The directions of the light sources were recovered from the mirror sphere using bright point clustering and simple geometry. Fast shutter speed was used to avoid intensity saturation in the acquired images of mirror sphere for estimating the relative strengths of different light sources. A method to recover the light distribution of a natural environment from a mirror sphere and how to cluster them into discreet directional sources is discussed in [20].

Because our algorithm assumes the surface is made of a single material, we manually identify a part of the mouse surface that has a single shiny finish. 3 of the 11 input images acquired are shown in Fig. 4.

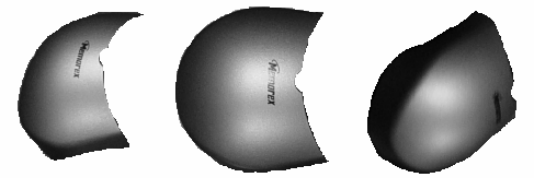

**Fig. 4 3 input images in the mouse surface data set**

Fig. 5 shows the synthesized images after the iterative optimization at first (coarse) and second (after the subdivision) scale. We can see that the estimated shape converges to the correct shape. Most of the surface variation is captured. The only problem area is the lower right corner of the segmented surface, which is smoothed out by the algorithm. These high curvature corners are difficult to reconstruct since they cannot generate enough image differences to push the vertices to the correct positions. The estimated reflectance is quite close to the input images.

In Table 1., we list the estimated Phong model parameters at two scales and the extrapolated Phong parameters.

We also synthesize 10 new views of the mouse surface with estimated shape and reflectance parameters and compare them with the captured images. These views are not used in the estimation. Fig. 6 shows the Average Absolute Image Difference (AAID) over the object area in each view between

synthesized images and the ground truth. Wrong estimates of reflectance, as well as incorrect or missing parts of surface shape will lead to large AAID values.

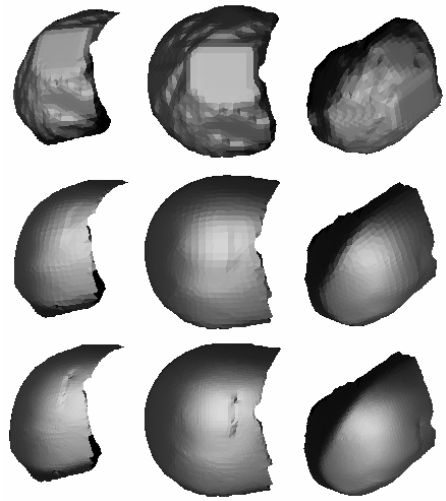

**Fig. 5 Synthesized images after each reflectance model Optimization. 1st row: Optimized reflectance model with the initial shape. 2nd row: Optimization result at 1st scale. 3rd row: Optimization result at 2nd scale.**

**Table 1. Estimated Phong model parameters**

| | Estimated | | Normalized | | |
|---|---|---|---|---|---|
| | kd | Ks | kd | Ks | $\alpha$ |
| 1st scale | 0.089 | 0.324 | 0.215 | 0.785 | 3.81 |
| 2nd scale | 0.094 | 0.357 | 0.208 | 0.792 | 4.18 |
| extrapolated | 0.099 | 0.390 | 0.201 | 0.799 | 4.55 |

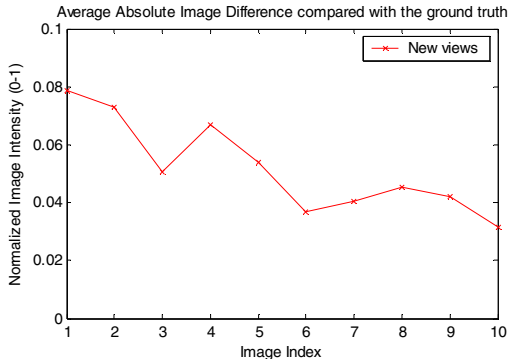


**Fig. 6 Average Absolute Image Difference between intensities of objects in the synthesized images for 10 new views (image index) using the estimated shape and reflectance model parameters, and the corresponding intensities in the 10 ground truth images.**

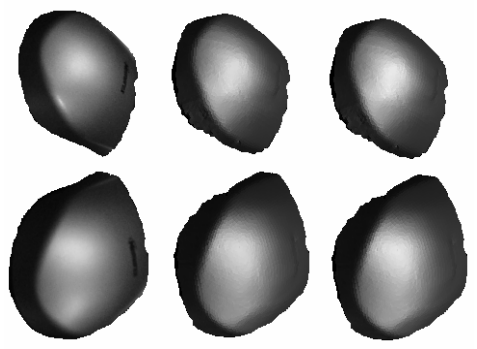

(1) (2) (3)

**Fig. 7 Synthesized images in two new views. (1) Original Images (2) Synthesized images with estimated shape and Phong parameters at 2nd scale (3) Synthesized new views with the same shape but extrapolated Phong parameters.**

Fig. 7 shows two synthesized new views for visual verification. Note that the surface reflectance is not as sharp as the original image, which means the estimated Phong exponent is smaller than the actual value. Similar blurring effect can also be observed in other work [12] when they estimate the reflectance model of a shinny surface. The light estimation error and camera calibration error can be two major reasons for this. The approximation of the surface normals inside a triangle with a single one in our algorithm also contributes to the blur. We can see from Table 1 and Fig. 7 that Richardson extrapolation makes the specular part a little bit sharper.

### 4.2 The enfant data set

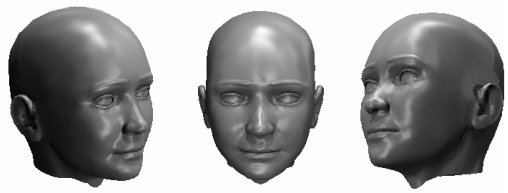

**Fig. 8 3 input images in the enfant data set**

The enfant data set consists of 12 views placed around a computer-rendered human head model made from a single material. 3 of the input images are shown in Fig 8. There are a total of 20 directional light sources which comprise a fairly complicated lighting environment. Note there are shadow areas on and under the nose, and around the eyes. We assume the camera parameters and lighting distributions are known.

We ran the minimization process at two different scales and the optimization results at first (coarse) and second (after the subdivision) scale are shown in Fig. 9. We can see that the estimated shape converges to the correct model, and at the finer scale more face features can be recovered. Also the shadows on and under the nose area are correctly synthesized. The reader may notice that the ears are not well reconstructed. This is again due to the high curvature of the ears. Also the concavity in the back of the ear does not follow the star-shape constraint we assume.

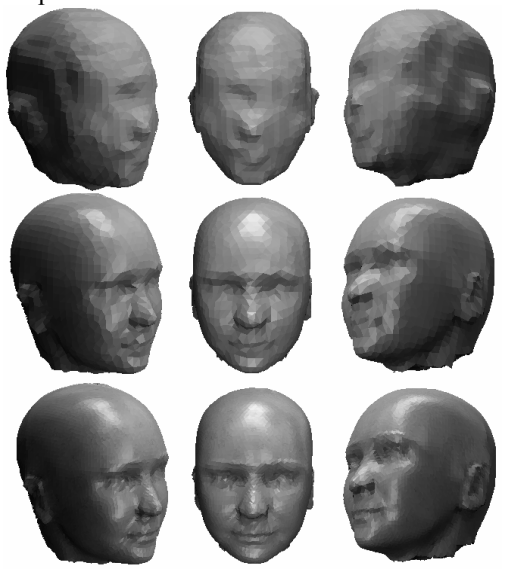

**Fig. 9 Synthesized images after each reflectance model optimization. 1st row: Optimized reflectance model with the initial shape. 2nd row: Optimization result at 1st scale. 3rd row: Optimization result at 2nd scale.**

**Table 2. Estimated Phong model parameters**

| | Estimated | | Normalized | | |
|---|---|---|---|---|---|
| | $k_d$ | $k_s$ | $k_d$ | $k_s$ | $\alpha$ |
| 1st scale | 1.099 | 1.415 | 0.437 | 0.563 | 24.4 |
| 2nd scale | 1.083 | 1.661 | 0.395 | 0.605 | 28.1 |
| extrapolated | 1.067 | 1.907 | 0.359 | 0.641 | 31.8 |
| Ground Truth | - | - | 0.364 | 0.636 | 32.0 |

**Table 3. Estimated Phong parameters using different mesh sizes (Exp. 1 is 25% larger, and Exp. 2 is 25% smaller)**

| Experiments | | Estimated | | Normalized | | |
|---|---|---|---|---|---|---|
| | | $k_d$ | $k_s$ | $k_d$ | $k_s$ | $\alpha$ |
| 1 | 1st scale | 1.102 | 1.366 | 0.447 | 0.554 | 25.4 |
| | 2nd scale | 1.087 | 1.696 | 0.391 | 0.609 | 29.8 |
| | Extrapolated | 1.073 | 2.026 | 0.346 | 0.654 | 34.1 |
| 2 | 1st scale | 1.099 | 1.443 | 0.432 | 0.568 | 24.4 |
| | 2nd scale | 1.080 | 1.701 | 0.388 | 0.612 | 28.1 |
| | Extrapolated | 1.062 | 1.958 | 0.352 | 0.648 | 31.7 |

The estimated and the ground truth values of Phong model parameters are listed in Table 2. We can see that with the decrease of triangle size, the estimated Phong parameters get closer to the ground truth. Richardson extrapolation gives even better estimates.

To test the effectiveness of the Richardson Extrapolation, we performed two additional experiments using two different initial mesh sizes: one was 25% larger and another was 25% smaller than used in the previous experiment. Recovered Phong parameters at each scale as well as the extrapolated results are shown in Table 3. In both experiments, the Richardson extrapolation gives noticeable improvements.

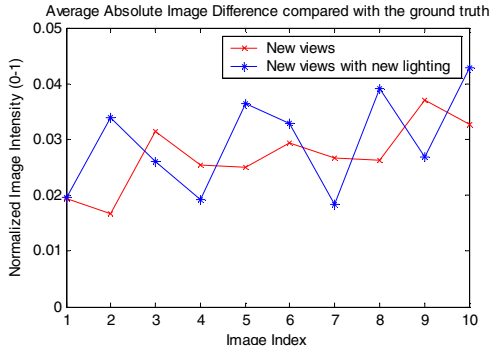


**Fig. 10 Average Absolute Image Difference between intensities of objects in the synthesized images for 10 new views (image index) using the estimated shape and reflectance model parameters, and the corresponding intensities in the 10 ground truth views.**

(1) (2) (3)

**Fig. 11 Images from a new viewpoint but using the same illumination (1st row) and under a different illumination (2nd row) compared with ground truth. (1) Ground truth images (2) Synthesized images using estimated shape and Phong parameters at 2nd scale (3) Synthesized image with the same shape but extrapolated Phong parameters.**

We synthesized images with estimated shape and reflectance model parameters from 10 new viewing directions, using the same illumination as well as a new illumination. The results are compared with the ground truth and summarized in Fig. 10. Fig. 11 Shows images from one of these views for visual comparison.

## 5. Conclusion and future work

We have proposed an algorithm that can estimate shape and reflectance parameters simultaneously from multiple views of an object made of a single material with lighting known or measured separately. We represent the object shape using triangular mesh and use the Phong reflectance model to compute the reflectance of each triangle. We proposed an iterative method to find optimal shape and reflectance parameters to minimize the difference between synthesized images and the observed images. The algorithm can handle self-occlusion and self-shadowing. We also propose the use of Richardson extrapolation to refine the reflectance model estimation beyond that allowed by recursive triangle subdivision. Experiment results on synthetic and real data show that the algorithm is effective in recovering both the 3D shape and reflectance parameters of non-lambertian objects.

Our future work will focus on extending the algorithm to objects that consist of multiple materials. Also we are attempting to eliminate the need for explicit lighting estimation.

## 6. Acknowledgements

The support of the National Science Foundation under grant ECS 02-25523 is gratefully acknowledged. Tianli Yu is supported in part by a Beckman Institute Graduate Fellowship.

## 7. References

[1] H. Jin, S. Soatto, A. Yezzi, "Multi-view stereo beyond Lambert", Computer Vision and Pattern Recognition, 2003. Proceedings, Vol. 1, pp 171-178, June 2003

[2] R. Zhang, P.S. Tsai, J. E. Cryer, and M. Shah, "Shape from Shading: A Survey", IEEE Trans. PAMI, Vol. 21, No. 8, pp 690-706, Aug. 1999

[3] J. Thomas, W. Kober, F. Leberl, "Multiple Image SAR Shape-from-Shading," Photogrammetric Engineering and Remote Sensing, vol. 57, no. 1, pp. 51-59, Jan 1991

[4] D. Samaras, D. Metaxas, P. Fua and Y. G. Leclerc, "Variable Albedo Surface Reconstruction from Stereo and Shape from Shading", Computer Vision and Pattern Recognition, 2000. Proceedings. Vol. 1, pp 480-487, June 2000

[5] K. M. Lee, C. J. Kuo, "Shape from Shading with a Generalized Reflectance Map Model", Computer vision and image understanding, Vol. 67, No. 2, pp. 143–160, Aug. 1997

[6] A. Hertzmann, S. Seitz, "Shape and Materials by Example: A Photometric Stereo Approach", Computer Vision and Pattern Recognition, 2003. Proceedings. Vol. 1, pp. 533-540, June 2003

[7] S.R. Marschner, "Inverse Rendering for Computer Graphics," Ph.D. Thesis, Cornell University, Aug. 1998.

[8] P. Debevec, T. Hawkins, C. Tchou, H.P. Duiker, W. Sarokin, and M. Sagar. "Acquiring the reflectance field of a human face", Proceedings of the 27th annual conference on Computer graphics and interactive techniques, pages 145–156. 2000

[9] R.C. Love. "Surface Reflection Model Estimation from Naturally Illuminated Image Sequences", PhD thesis, The University of Leeds, Sep. 1997.

[10] J. I. Apricio, J.G.Garcia-Bermejo, "An Approach for Determining Phong Reflectance Parameters from Real Objects," Pattern Recognition, 2000. Proceedings. 15th International Conference on, pp. 568 -571 vol.3 Sept. 2000

[11] R. Ramamoorthi and P. Hanrahan, "A Signal-Processing Framework for Inverse Rendering", Proceedings of the 28th annual conference on Computer graphics and interactive techniques, pp.117-128, 2001

[12] Y. Sato, M. D. Wheeler, and K. Ikeuchi. "Object shape and reflectance modeling from observation", Proceedings of the 24th annual conference on Computer graphics and interactive techniques, pages 379–388, 1997.

[13] T.E. Kim, H.K. Hong, J.S. Choi, "Estimation of hybrid refectance properties and shape reconstruction using the LMS method", Pattern Recognition, 33 (2000), pp 161-171

[14] H. Schultz, "Retrieving shape information from multiple images of a specular surface," IEEE Trans. PAMI, Vol 16, No. 2, pp 195-201 Feb. 1994

[15] B. T. Phong. "Illumination for Computer Generated Pictures," Commun. of the ACM, vol.18, no.6, Jun. 1975

[16] S. K. Nayar, K. Ikeuchi, and T. Kanade, "Shape from Interreflections," International Journal of Computer Vision, Vol. 6, No. 3, pp. 173-195, 1991.

[17] Matlab Optimization Toolbox, The MathWorks, Inc. http://www.mathworks.com/products/optimization/

[18] Michael T. Heath, Scientific Computing, An Introductory Survey, Second Edition, McGraw-Hill, New York, 2002

[19] J. Y. Bouguet, Camera Calibration Toolbox for Matlab http://www.vision.caltech.edu/bouguetj/calib_doc/

[20] High Dynamic Range Image Processing and Manipulation, http://www.debevec.org/HDRShop/

[21] J. Y. Aloimonos, D. Shulman, Integration of Visual Modules, Ch 3 Shape from Shading and Motion, Academic Press, San Diego CA, 1989